

# Tailored Coupled Cluster Theory in Varying Correlation Regimes

Maximilian Mörchen<sup>a</sup>, Leon Freitag<sup>a,b</sup>, and Markus Reiher<sup>a,1</sup>

<sup>a</sup> ETH Zürich, Laboratorium für Physikalische Chemie, Vladimir-Prelog-Weg 2,  
8093 Zürich, Switzerland

<sup>b</sup> Universität Wien, Institut für theoretische Chemie, Währinger Str. 17,  
1090 Vienna, Austria

09.10.2020

## Abstract

The description of strongly correlated electrons within the framework of coupled cluster theory still poses challenges in electronic structure theory. The tailored coupled cluster (TCC) approach is a promising *ansatz* that preserves the simplicity of single-reference coupled cluster theory, while incorporating a multi-reference wave function through amplitudes obtained from a preceding multi-configurational calculation. Here, we present a detailed analysis of the TCC wave function based on model systems, which require an accurate description of both static and dynamic correlation. We investigate the reliability of the TCC approach with respect to the exact wave function obtained by full configuration interaction in the orbital space given. In addition to the error in the electronic energy and  $T_1$  and  $D_1$  diagnostics, we exploit the overlap of TCC and full configuration interaction wave functions as a quality measure. Based on these diagnostics, we critically review the advantages and drawbacks of TCC. We find this model to be promising in calculations on well chosen, balanced active orbital spaces, even if they become large and therefore require modern active-space approaches that are not restricted to comparatively small orbital numbers.

---

<sup>1</sup>Corresponding author; e-mail: markus.reiher@phys.chem.ethz.ch; ORCID: 0000-0002-9508-1565

# 1 Introduction

The solution of the time-independent electronic Schrödinger equation within a finite orbital basis is given by a many-body expansion called Full Configuration Interaction (FCI). Since FCI includes every possible configuration within the many-electron Hilbert space constructed of the pre-defined orbital basis, it delivers the exact wave function in the finite basis set, but scales exponentially with the number of orbitals. The simplest way to achieve polynomial scaling is the truncation of the FCI expansion in a systematic manner, typically defined in terms of a maximum 'excitation' level, which measures the maximum number of orbital substitutions in some reference determinant. Qualitatively speaking, to recover the decisive correlation energy [1] after an HF calculation, excited determinants must be included in the wave function expansion.

In contrast to FCI, which is invariant under a linear transformation of the orbitals, truncated CI depends on the particular choice of reference determinant. This reference is usually the Hartree-Fock (HF) determinant, in which, in a closed-shell case, the energetically lowest canonical HF orbitals are doubly occupied with electrons. A consequence of the truncation is that truncated CI lacks important features of a reliable wave function such as size-consistency and size-extensivity [2]. By contrast, the coupled cluster (CC) *ansatz* [3–6] restores these important properties through its exponential expansion, even at a truncated level [7, 8]. CC including single and double excitations [9] (CCSD) and perturbative triples (CCSD(T) [10, 11]) provides an excellent compromise of accuracy and cost, which is why it is referred to as the *gold standard* in computational quantum chemistry.

It is desirable to include the most important determinants of arbitrary excitation level in a CI expansion in a systematic and well-defined manner. Since it is not clear which and how many of such determinants there will be, it is convenient to prune the orbital space to a subspace, which is referred to as the complete active space (CAS), in which FCI is still feasible. Obviously, active space methods such as CASCI and CAS self-consistent field (CASSCF)[12] are also constrained by ex-

ponential scaling and by a lack of dynamic correlation as no excitations outside of the active space are considered. The introduction of the Density Matrix Renormalization Group (DMRG) [13, 14] to quantum chemistry [15–29] made considerably larger active spaces accessible due to a decomposition of the CI coefficient tensor that brings about polynomial scaling. Another powerful new large-CAS method emerged in the past decade: the FCI Quantum Monte Carlo (FCIQMC) approach [30, 31] in which the wave function’s coefficient tensor is represented by *walkers*.

Large active spaces accessible by FCIQMC and DMRG recover more dynamic correlation in the active space, although the majority of this type of electron correlation would be missed in typical calculations where far more virtual orbitals are still excluded from the active space. To then recover the still lacking dynamic correlation is a major challenge because all post-diagonalization methods available for that purpose are approximate compared to the dynamic correlation in the active space evaluated by exact diagonalization. To avoid an imbalance in the description of dynamic correlation, one is advised to choose a small active space of all strongly entangled orbitals and leave the dynamic correlation for a consistent separate treatment.

Since quantum chemical approaches for strong electron correlation problems are usually active space methods, they separate the orbital space into two parts — a comparatively small one that collects (near-)degenerate and highly entangled orbitals in the active space [32–36] and a large one comprising the rest of the virtual orbitals. As a consequence, electron correlation is divided into two classes: (1) dynamic correlation, which can be recovered by including (highly) excited determinants from the entire orbital space [37], and (2) static correlation, caused by (near-degenerate) determinants, which have a large weight in the wave function [38].

The standard CC approach depends on a single reference (SR) determinant. Hence, it is not suited for systems with strong static correlation. In other words, for molecular systems where HF provides a good approximation — e.g., for the ground state of many organic molecules in their equilibrium structure, SRCC will work accurately. However, for many chemical problems such as bond-breaking processes, ex-

cited states, and open-shell transition metal as well as rare earth complexes, SRCC will become inaccurate and may fail [39]. These types of problems require several reference determinants to be used as a reference for the many-body expansion of the wave function.

A way to combine static and dynamic correlation with polynomial cost are multi-reference (MR) methods. The most common MR method is MRCI [40], in which, initially, a reference space is defined that aims to comprise the most important excitations. From these determinants, a truncated CI expansion is performed which includes excitations into the entire Hilbert space up to the truncation level. Since MRCI is neither size-consistent nor size-extensive, MRCC approaches have been developed as a way out of these problems [2, 41, 42].

Current MRCC approaches can be divided into two main classes: (i) internally contracted and (ii) Jeziorski-Monkhorst [43]. One problem of both classes was the *multiple-parentage* problem [42] (the redundant description of amplitudes). By formulating ic-MRCC as universal valence theory in Fock space [44, 45] and JM-MRCC as state universal theory in Hilbert space [43, 46], the redundant description could be circumvented. However, both classes suffer from numerical instabilities, due to intruder states which are caused by (near-)degenerate determinants [47, 48]. Another drawback of JM-MRCC theories is the limitation of the CAS size, because these approaches have increasing problems for increasing active space sizes [49].

Implementations of ic-MRCCSD and ic-MRCCSDT without any approximation were presented by Evangelista and Gauss [50] and by Hanauer and Köhn [51], respectively. The ic-MRCC method has the advantage of featuring roughly the same number of cluster operators as single-reference CC. This makes it well suited for large active spaces, although typically small active spaces are used for feasibility reasons, which may create a problem for the optimized orbital basis if the active space is overly restricted. ic-MRCCSD calculations are expensive and require elements of the 5-body reduced density matrix. However, it can be made invariant with respect to orbital rotations in core, active, and virtual space and the reference wave function can be optimized self-consistently. Nevertheless, the cluster operators

do not commute, since they can create and annihilate electrons in the active space. Hence, the BCH series does not truncate naturally. Another problem are the average treatment of electron correlation and the redundant description of excitations, which have to be removed by linear transformation.

Canonical transformation (CT) theory [52, 53] corresponds to the class of ic-MRCC theories that is applicable to large active spaces. The idea behind CT is a cumulant expansion of operators [54]. However, the main problem in CT theory is that the cumulant expansion cannot become exact in the limit due to an unbalanced treatment of some of the terms. Another drawback of this method is the slow convergence of the expansion so that many recursive commutator iterations are required which results in computational cost that are not pre-determinable.

In view of the issues with MRCC approaches, the most common methods to combine static and dynamic correlation are still multi-reference configuration singles ('S') and doubles ('D') with a Davidson correction ('+Q'), i.e., MRCISD+Q [40, 55, 56] and multi-reference perturbation theory (MRPT) [57–59], which both come also with significant drawbacks and immense costs (all require elements of higher-order density matrices — up to 4- and 5-body terms). MRCISD+Q uses a truncated CI expansion so that the resulting wave function lacks the same properties that truncated CI itself lacks. MRPT is a perturbation *ansatz* and requires large basis sets to describe the electron cusp properly; typically it poorly describes long-range dynamic correlation. A conceptually simpler alternative to *genuine* MRCC methods are MR-driven SRCC approaches introduced by Oliphant and Adamowicz [60], where an SRCC wave function is externally corrected by another MR wave function. These approaches are based on a single reference only, but include excitations from an active space, a procedure that introduces static correlation effects into an SRCC wave function.

Specialized CC variants have been proposed that may alleviate some problems of single-reference CC. For instance, the completely renormalized CC (CR-CC) theory is a special case of the method of moments CC (MM-CC) approach, where the perturbative correction is renormalized by a functional which scales with fully described CC amplitudes [61–63]. However, it can be seen that even CR-CCSD(TQ),b, which

is based on CCSD(T) and improves the corresponding CCSD(TQ) or CCSD(TQ<sub>f</sub>), may sometimes show an unphysical behavior in the dissociation limit.

Another MR-driven SRCC *ansatz* introduced by Kinoshita, Hino, and Bartlett is Tailored CC (TCC) [64]. In its singles and doubles variant, TCCSD, CI coefficients for singly and doubly excited determinants are first extracted from a CAS wave function and then transformed to CC amplitudes. The CAS state parameters included in this way in an SRCC wave function are kept frozen so that they *tailor* the remaining CC amplitudes during their optimization. TCCSD was used by Hino *et al.* to calculate the equilibrium structure of ozone and its vibrational frequencies [65]. Later, Lyakh, Lotrich, and Bartlett also included perturbative triples into the TCCSD wave function for the calculation of the automerization of cyclobutadiene [66]. Since TCC prevents relaxation of the CAS coefficients, they are decoupled from the CC amplitudes. To improve on the quality of the CAS coefficients, Melnichuk and Bartlett used an extended active space to include more orbitals in the optimization of the CAS [67, 68]. Naturally, this way of letting the state parameters responsible for static correlation see more of the dynamic correlation points toward CAS approaches that allow for truly large active spaces, i.e., FCIQMC and DMRG. It was Veis *et al.* who introduced the TCC concept to DMRG [69]. Based on the DMRG-TCC approach, Faulstich *et al.* provided a mathematical analysis in which they formally derived its advantages and disadvantages [70]. Subsequently, these authors presented a numerical DMRG-TCC study at the example of dinitrogen dissociation, which focused on the DMRG in TCCSD[71].

In view of the salient properties of TCC and the fact that the above-mentioned analyses have not considered an analysis of the CC part of the wave function or a comparison with FCI, we intend to close this gap in the present paper. We will examine the TCCSD method at the example of well-known model systems that require static and dynamic correlation. Due to the small size of these systems, FCI calculations are possible, so that we have access to the best possible wave function. Since, the energy does not provide good diagnostics for the quality of the wave function, additionally  $T_1$  and  $D_1$  diagnostics [72–74] as well as the overlap of the TCC

wave function with FCI are shown in this work.

## 2 Theory

### 2.1 Single-Reference Coupled Cluster

The SRCC wave function is defined by

$$|\Psi_{\text{CC}}\rangle = e^{\hat{T}}|\Phi_0\rangle, \quad (1)$$

where the cluster operator  $\hat{T}$  denotes to a linear combination of cluster operators  $\hat{T}_\nu$  of excitation level  $\nu$ . The exponential can be Taylor expanded and the truncated SRCC is then size-consistent and size-extensive [7, 8]. Another advantage of this *ansatz* is the faster convergence to the FCI limit than truncated CI — despite the fact that the amplitude equations are not solved variationally but by projection.

The cluster operator is defined as

$$\hat{T}_\nu = \frac{1}{(\nu!)^2} \sum_{\substack{a_1, \dots, a_\nu \\ i_1, \dots, i_\nu}} t_{i_1, \dots, i_\nu}^{a_1, \dots, a_\nu} \hat{a}_{a_1}^\dagger \dots \hat{a}_{a_\nu}^\dagger \hat{a}_{i_1} \dots \hat{a}_{i_\nu}, \quad (2)$$

where  $a_p^\dagger$  and  $a_q$  are creation and annihilation operators and  $t_{i_1, \dots, i_\nu}^{a_1, \dots, a_\nu}$  represents the amplitude for the corresponding excitation. The indices  $p, q, r, \dots$  represent generic orbitals, while  $i, j, k, \dots$  and  $a, b, c, \dots$  correspond to hole and particle indices, respectively. The amplitudes in SRCC are optimized by the amplitude equation

$$0 = \langle \Phi_\nu | e^{-\hat{T}} \hat{H} e^{\hat{T}} \Phi_0 \rangle, \quad (3)$$

whereby an excited determinant  $\Phi_\nu$  is projected onto the similarity transformed Hamiltonian  $e^{-\hat{T}} \hat{H} e^{\hat{T}}$  acting on the reference determinant  $\Phi_0$ . Because of the similarity transformation, the Hamiltonian is no longer Hermitian. The advantage of this formulation is the natural truncation of the Baker-Campbell-Hausdorff series after the 4-fold commutator. With the optimized amplitudes, the SRCC energy can be evaluated as follows

$$\langle \Phi_0 | e^{-\hat{T}} \hat{H} e^{\hat{T}} \Phi_0 \rangle = E_{\text{CC}}. \quad (4)$$

## 2.2 Tailored Coupled Cluster

TCC combines an active space method with SRCC leading to a formulation that is supposed to describe the static and the dynamic correlation of a system [64]. Since the coefficients from an active space are not optimized during the SRCC process, TCC corresponds to the class of externally corrected CC theories. The TCC wave function employs the split-amplitude *ansatz* [75], which means that the linear expansion of the cluster operators  $\hat{T}_\nu$  is divided into operators that act either on the active ('CAS') or on the external ('ext') space,

$$|\Psi_{\text{TCC}}\rangle = e^{\hat{T}}|\Phi_0\rangle = e^{(\hat{T}^{\text{ext}}+\hat{T}^{\text{CAS}})}|\Phi_0\rangle = e^{\hat{T}^{\text{ext}}}e^{\hat{T}^{\text{CAS}}}|\Phi_0\rangle. \quad (5)$$

Because  $\hat{T}^{\text{ext}}$  and  $\hat{T}^{\text{CAS}}$  never include the same set of orbitals and act on a single reference determinant, the operators commute with each other [64]. In the TCCSD variant, CCSD is corrected by the singly and doubly excited CAS amplitudes.

The excitation of the CAS coefficients is defined with respect to a reference determinant, which must be the same as for the CC expansion.

Therefore, the TCCSD wave function

$$|\Psi_{\text{TCCSD}}\rangle = e^{(\hat{T}_1^{\text{ext}}+\hat{T}_2^{\text{ext}})}e^{(\hat{T}_1^{\text{CAS}}+\hat{T}_2^{\text{CAS}})}|\Phi_0\rangle \quad (6)$$

contains the single and double excitations from both spaces, implying that the coefficients of higher excitations in the CAS are neglected in the TCC approach. Hence, TCCSD includes the same excitations as (SR)CCSD, where the CAS amplitudes are frozen during the optimization of the external amplitudes [64]. Moreover, the TCCSD wave function has the same number of parameters as the analogous SR-CCSD wave function so that the computational scaling is comparable. Compared to a *genuine* MRCC, the TCC approach therefore has the advantage that problems, which are related to multiple reference determinants such as the *multi-parantage* problem, do not occur. If the active space amplitudes were allowed to relax, they would converge to the corresponding CCSD amplitudes and would have no corrective effect on the external amplitudes.



The CI coefficients from the CAS calculation, which correspond to single and double excitations, must be transformed into CC amplitudes based on the relationship between cluster,  $\hat{T}$ , and CI,  $\hat{C}_i$ , operators

$$\begin{aligned}\hat{T}_1^{\text{CAS}} &= \hat{C}_1, \\ \hat{T}_2^{\text{CAS}} &= \hat{C}_2 - \frac{1}{2} [\hat{C}_1]^2.\end{aligned}\tag{7}$$

In the case of a CI wave function that is not intermediate-normalized, i.e.  $\langle \Psi_{\text{CAS}} | \Phi_{\text{HF}} \rangle = 1$ , the transformation to CC amplitudes requires normalization by the coefficient  $c_0$ , which corresponds to the reference determinant:

$$\begin{aligned}t_i^a &= \frac{c_i^a}{c_0}, \quad a, i \in \text{CAS}, \\ t_{ij}^{ab} &= \frac{c_{ij}^{ab}}{c_0} - \frac{(c_i^a c_j^b - c_i^b c_j^a)}{c_0^2}, \quad a, b, i, j \in \text{CAS}.\end{aligned}\tag{8}$$

Because the exact ('full') CC energy depends only on single and double amplitudes (calculated in the presence of all higher-excited amplitudes from the amplitude equations) and as we calculate the single and double amplitudes from an FCI in a CAS, i.e., also under the condition that they are exact from a full CC point of view, we can calculate the CAS energy with a CCSD *ansatz* exploiting the amplitudes obtained from the CASCI calculation. Hence, the CAS energy is obtained after the transformation of the coefficients by

$$\langle \Phi_0 | \hat{H} e^{\hat{T}^{\text{CAS}}} \Phi_0 \rangle_c = E_{\text{CAS}},\tag{9}$$

where  $c$  means that only connected terms are involved [64]. Since the CAS amplitudes replace the corresponding CCSD amplitudes, the external cluster operators must be redefined as

$$\begin{aligned}\hat{T}_1^{\text{ext}} &= \sum_{a,i} t_i^a \hat{a}_a^\dagger \hat{a}_i, \quad \{a, i\} \not\subset \text{CAS}, \\ \hat{T}_2^{\text{ext}} &= \frac{1}{4} \sum_{a,b,i,j} t_{ij}^{ab} \hat{a}_a^\dagger \hat{a}_b^\dagger \hat{a}_j \hat{a}_i, \quad \{a, b, i, j\} \not\subset \text{CAS}\end{aligned}\tag{10}$$

to prevent external excitation within the CAS space. This implies that excitations from the external to the active space and vice versa are part of the external ampli-

tudes. Hence, the amplitude equations of the TCCSD formalism are defined as

$$\begin{aligned}\langle \Phi_i^a | \hat{H} e^{(\hat{T}_1^{\text{ext}} + \hat{T}_2^{\text{ext}})} e^{(\hat{T}_1^{\text{CAS}} + \hat{T}_2^{\text{CAS}})} \Phi_0 \rangle_c &= 0, \quad \{a, i\} \not\subset \text{CAS}, \\ \langle \Phi_{ij}^{ab} | \hat{H} e^{(\hat{T}_1^{\text{ext}} + \hat{T}_2^{\text{ext}})} e^{(\hat{T}_1^{\text{CAS}} + \hat{T}_2^{\text{CAS}})} \Phi_0 \rangle_c &= 0, \quad \{a, b, i, j\} \not\subset \text{CAS},\end{aligned}\tag{11}$$

Only the external space amplitudes are optimized and the pre-calculated CAS amplitudes encode the static correlation in the system. The electronic correlation energy is obtained as a sum of the active space energy  $E_{\text{CAS}}$  and the remaining external energy  $E_{\text{ext}}$  by

$$\langle \Phi_0 | \hat{H} e^{(\hat{T}_1^{\text{ext}} + \hat{T}_2^{\text{ext}})} e^{(\hat{T}_1^{\text{CAS}} + \hat{T}_2^{\text{CAS}})} \Phi_0 \rangle_c = E_{\text{CAS}} + E_{\text{ext}} = E_{\text{TCCSD}}.\tag{12}$$

As it has been shown by Lyakh *et al.* [66], TCCSD can be supplemented with a perturbative triples correction. For its evaluation it is crucial to exclude every triple-excited amplitude which depends purely on CAS singles and doubles.

In this work, we consider an analysis of TCCSD without any perturbative correction, because (i) this has been the standard TCC model so far and (ii) it is not plagued by additional computational burden (noting though that such a correction may still be decisive for a truly reliable TCC approach). We will turn to triples corrections in the TCC framework in future work.

## 2.3 Diagnostic descriptors

### 2.3.1 $c_0$ coefficient

As a first estimation of the MR character of a wave function, the CI coefficient  $c_0$ , which corresponds to the reference determinant, can be taken into account. If the HF determinant is a good approximation of the system, the  $c_0$  coefficient should be close to one for a normalized wave function.

### 2.3.2 $T_1$ norm

Unfortunately, the  $c_0$  coefficient is useless as a diagnostic for intermediate normalized wave functions, because the overlap with the reference determinant is always one. Therefore, for SRCC wave functions the  $T_1$  and  $D_1$  diagnostics [72–74], which are independent of the  $c_0$  coefficient, may be used to assess the reliability of a CI or CC wave function. The weighted  $T_1$  norm is defined as

$$T_1 = \sqrt{\frac{\vec{t}_1 \cdot \vec{t}_1}{N}}, \quad (13)$$

where the vector  $\vec{t}_1$  contains all single amplitudes and  $N$  represents the number of electrons. The number of single-excitation CC amplitudes increases with the number of electrons  $N$ . Hence, the Euclidean norm of the amplitudes is divided by  $\sqrt{N}$  to make  $T_1$ -diagnostics independent of the number of electrons. The threshold value for  $T_1$  that points to a reliable CC wave function is 0.02 [73].

### 2.3.3 $D_1$ norm

Owing to the sensitivity of  $T_1$  diagnostics to orbital rotations, the  $D_1$  norm was introduced as

$$D_1 = \sqrt{\lambda_{\max}(\mathbf{T}\mathbf{T}^\dagger)}, \quad (14)$$

where  $\mathbf{T}$  represents the single-excitation amplitude matrix, where the columns and rows correspond to holes and particles, respectively.  $\lambda_{\max}$  is the largest eigenvalue of the matrix  $\mathbf{T}\mathbf{T}^\dagger$ . The threshold value of  $D_1$  to classify a CC wave function as reliable is 0.05 [74]. By virtue of the diagonalization of  $\mathbf{T}\mathbf{T}^\dagger$ , the  $D_1$  norm is less sensitive to orbital rotations.

### 2.3.4 Energy and Overlap error

The most reliable assessment of an approximate theory is a comparison with FCI in the same orbital basis. Since the CC equations are solved by projection, we define

an energy error in terms of FCI for a test wave function indicated by the subscript  $x$  as

$$\Delta E = |\langle \Psi_{\text{FCI}} | \hat{H} | \Psi_{\text{FCI}} \rangle - \langle \Phi_0 | \hat{H} | \Psi_x \rangle|. \quad (15)$$

A second option for a direct comparison is one based on the wave function itself, e.g. in terms of the norm suggested by Kutzelnigg[76]

$$||\Psi_x - \Psi_{\text{FCI}}||^2 = 2(1 - \langle \Psi_{\text{FCI}} | \Psi_x \rangle). \quad (16)$$

The norm vanishes when  $\Psi_x$  becomes exact. In this work, we exploit the overlap error

$$\Delta_{\text{ov.}} = |1 - \langle \Psi_{\text{FCI}} | \Psi_x \rangle| \quad (17)$$

as a measure for the accuracy of a wave function. Obviously, the prohibitively steep scaling of FCI prevents us from exploiting energy and overlap errors in routine calculations as standard diagnostics.

### 3 Results

For the investigation of the TCCSD wave function we chose the model systems P4 [77] and H8 [78] to analyze the behavior of the method in the statically and dynamically correlated regimes. We compare all TCSSD results with results obtained with its single-reference analog, SRCCSD (for the sake of brevity, we drop the prefix 'SR' in the following), and with FCI data as the exact result within the given orbital basis set. Because the wave function is more sensitive to errors than the energy,  $T_1$  and  $D_1$  diagnostics [72–74] and especially the overlap of wave functions are in the focus of our analysis.

Since TCCSD corresponds to the class of MR-driven SRCC methods, the wave function still depends on a single reference determinant. To assess the effect of the reference determinant on the quality of the TCCSD wave function, we performed all calculations twice, based on the two most dominant determinants.

Nevertheless, the orbital basis also greatly affects the wave function. Since TCCSD requires the choice of an active space, we evaluated every property in the HF and CAS optimized orbital basis for the sake of comparison.

### 3.1 Computational Methodology

All calculations were carried out with the PySCF program package [79]. This includes the calculation of integrals, the HF and CAS orbital optimization, as well as the CASCI, FCI and CCSD calculations. To ensure that the same orbital basis and CI expansion is used throughout this work, we interfaced our in-house TCCSD implementation with PySCF. For all calculations on the P4 and H8 model, we followed Jankowski *et al.* [77, 78] and chose DZP ( $4s1p/2s1p$ ) [80] and DZ ( $4s/2s$ ) basis sets [81, 82], respectively. The entanglement analysis in section 3.3.1 was performed with the AutoCAS program [34, 36, 83] that allows one to identify the most statically correlated orbitals [32, 34]. Such analysis is based on entanglement entropy measures[84–86] such as the one-orbital entropy

$$s_p(1) = - \sum_{\beta=1}^4 w_{\beta,p} \ln w_{\beta,p} \quad (18)$$

calculated from the eigenvalues of the  $p$ -the one-orbital reduced density matrix  $w_{\beta,p}$ , which can be obtained from elements of the one- and two-particle reduced density matrix [87] and the mutual information of two orbitals  $p$  and  $q$

$$I_{pq} = \frac{1}{2} [s_p(1) + s_q(1) - s_{pq}(2)] (1 - \delta_{pq}) \quad (19)$$

obtained from the corresponding two-orbital entropy

$$s_{pq}(2) = - \sum_{\beta=1}^{16} w_{\beta,pq} \ln w_{\beta,pq}. \quad (20)$$

### 3.2 P4 model

The P4 model [77] consists of two hydrogen molecules with a constant intramolecular distance of 2 Bohr. The two fragments are aligned parallel to each other, resulting

in a planar rectangular configuration with the distance between the two molecules determined by the parameter  $\alpha$  (see Figure 1). In principle, the P4 model has a compressed configuration for  $\alpha < 2$ , a square configuration for  $\alpha = 2$ , and a stretched configuration for  $\alpha > 2$ .

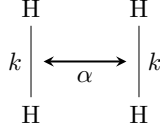


**Figure 1:** The P4 model in which  $\alpha$  is a parameter that is characteristic for the distance between the two  $\text{H}_2$  units and  $k$  is constant at 2 Bohr.

The stretched and compressed configurations have  $D_{2h}$  symmetry with the respective dominant determinants in short-hand notation (see supporting information for the complete set of HF orbitals)

$$|\Phi_1\rangle = |(1a_1)^2(1b_{2u})^2\rangle, \quad (21)$$

$$|\Phi_2\rangle = |(1a_1)^2(1b_{3u})^2\rangle, \quad (22)$$

while the quadratic configuration represents a degenerate case. The active space is defined by  $\text{CAS}(2e^-, (1b_{2u})(1b_{3u}))$ . The P4 model covers both SR and MR regimes. The MR character of the wave function can be tuned by the parameter  $\alpha$ . At large separation  $\alpha$  of the two molecules, size-consistency can be probed.

The importance of the individual determinants is evident from Figure 2. It becomes also clear that the use of  $\text{CAS}(2,2)$  orbitals, compared to HF orbitals, leads to no significant change of the  $c_0$  coefficient for the corresponding reference determinant.

$|\Phi_2\rangle$  represents the most dominant reference for the compressed configuration and  $|\Phi_1\rangle$  the one for the stretched configuration. Between  $1.75 < \alpha < 2.25$ , the wave function shows a significant multi-configurational character. These two determinants become completely degenerate at  $\alpha = 2$ . We denote determinants as  $\Phi_i$  and wave functions which depend on a reference  $i$  as  $\Psi_i$ . In the following, we study the

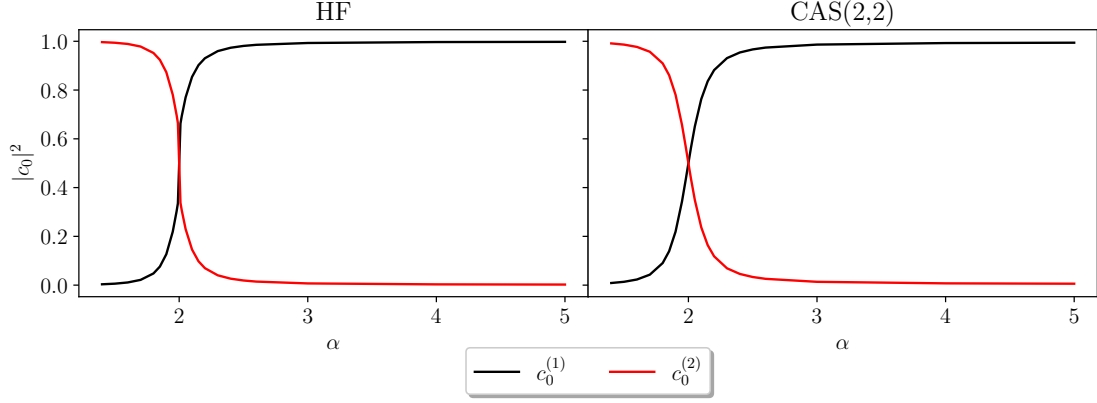


**Figure 2:** Square of the CI coefficient ( $|c_0|^2$ ) of  $\Phi_1$  ( $c_0^{(1)}$ ) and  $\Phi_2$  ( $c_0^{(2)}$ ) of Eqs. (21) and (22) for different values of  $\alpha$ . Both expansion coefficients were obtained for determinants constructed from different molecular orbital bases: (1) HF orbitals (left) and (2) CAS(2,2) orbitals (right).

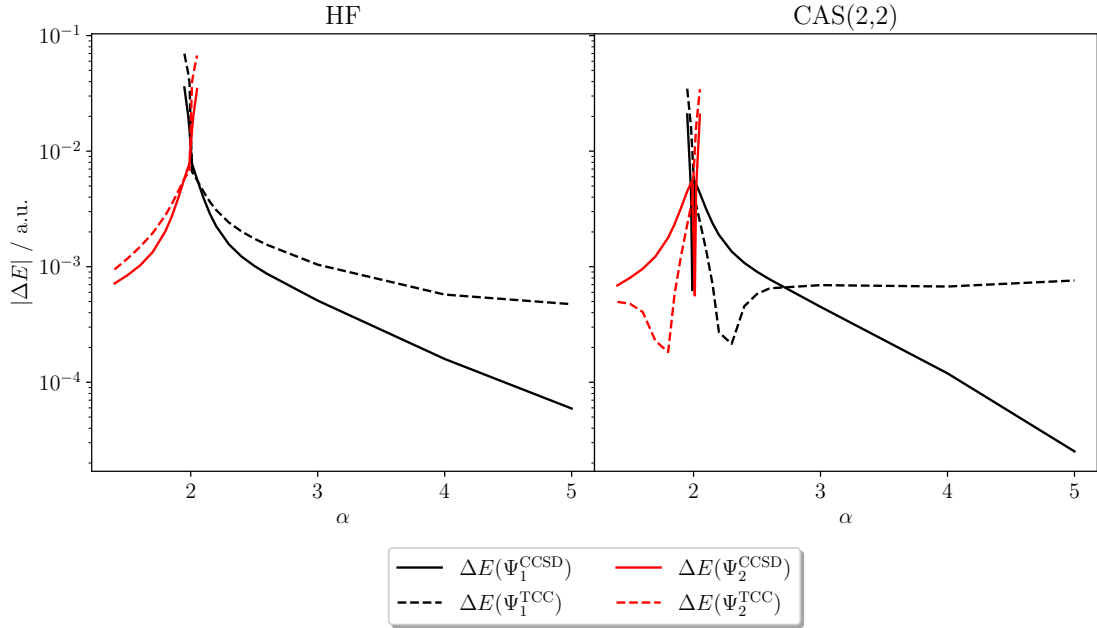


**Figure 3:** Absolute energy error  $|\Delta E|$  of TCCSD(2,2) and CCSD with respect to the FCI energy, based on the reference determinant  $\Phi_1$  and  $\Phi_2$  and different orbital bases: (1) HF orbitals (left) and CAS(2,2) orbitals (right).

reliability of the TCCSD and CCSD methods for different values of  $\alpha$ . We expect

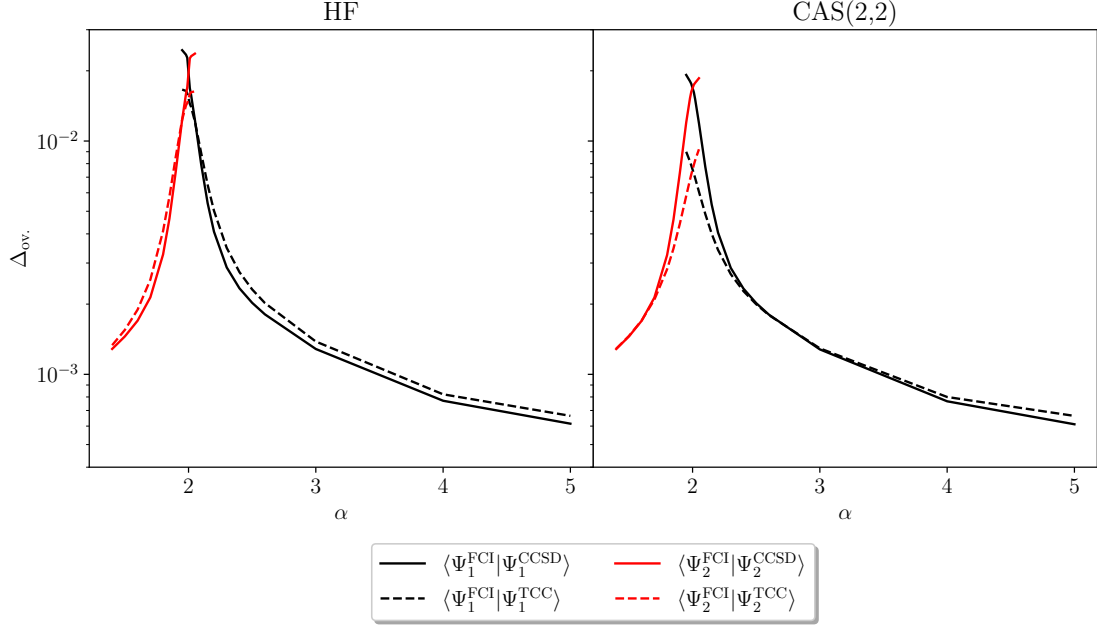
the reliability of CCSD to deteriorate as the determinant that was not chosen as the reference for CCSD starts to dominate in the wave function, while TCCSD should be able to describe the MR region qualitatively correct.

Figure 3 depicts the energy profile given as the absolute error with respect to the FCI energy (see supporting information for the potential energy surfaces). From this figure it is obvious that TCCSD is not a *genuine* MR method, since it shows a strong dependence on the reference, even if the most important orbitals are both included in the active space. Another problem is the energy error of the TCCSD in the SR region ( $\alpha < 1.75$  and  $\alpha > 2.25$ ), because it is still larger than the corresponding one for CCSD, when HF orbitals are used. Especially for the dissociated configuration ( $\alpha > 4.5$ ), the difference between TCCSD and CCSD gets larger, because TCCSD is, in contrast to CCSD, not size-consistent [69]. Only for the degenerate case, TCCSD leads to marginally better energies than CCSD. The reason for this is the qualitatively correct description by the amplitudes obtained from the active space. Since these amplitudes must not relax, they result in an improved energy compared to CCSD, while the total energy error is still unacceptable for an accurate MR description.

This situation changes in the CAS(2,2) optimized orbital basis, where TCCSD still shows a strong dependence on the dominant reference, but for the almost degenerate ones the energy error is smaller than for CCSD. Since the absolute error is shown and TCCSD is not variational, the decrease near the degenerate configuration is based on a sign change, which also explains the rapid increase of the error around  $\alpha \sim 2$ . For the dissociated configuration, due to size-consistency, the CCSD energy approaches FCI, while the error is nearly constant for TCCSD.

As already mentioned, the energy is not necessarily a benchmark for the quality of the wave function. A straightforward diagnostic for the quality of a wave function is its overlap with the FCI wave function. Figures 4 and 5 show the overlap error  $\Delta_{\text{ov}}$  of the CCSD and TCCSD wave function with the FCI wave function and with each other to highlight the reliability and differences between the two wave functions. For HF orbitals, both methods show a small overlap error in the SR-dominated





**Figure 4:** Overlap error  $\Delta_{\text{ov.}}$  of CCSD and TCCSD(2,2) with FCI, based on the reference determinants  $\Phi_1$  and  $\Phi_2$  and different orbital bases: (1) HF orbitals (left) and CAS(2,2) orbitals (right).

region for  $\alpha > 3$ . However, the overlap error increase for configurations, where the other determinant becomes more important. CCSD shows a similar behavior in the CASSCF(2,2) basis, while the overlap error for TCCSD(2,2) is significantly smaller for configurations with a larger MR character than in the HF basis.

In the HF orbital basis, CCSD shows a somewhat larger overlap with FCI than TCCSD. The largest difference between TCCSD and CCSD is again around  $\alpha = 2$ . The reason is the same as for the smaller energy error for the nearly degenerate configurations, when compared to CCSD. However, in TCCSD the external amplitudes are based on only one reference, which explains the increase of the overlap error for the degenerate configuration.

From the overlap between the CCSD and TCCSD wave function, it can be concluded that the wave functions for the SR-dominated cases differ only slightly, since the external amplitudes are based on the same reference as the CCSD and the active space amplitudes differ not as much from the corresponding ones in CCSD as for

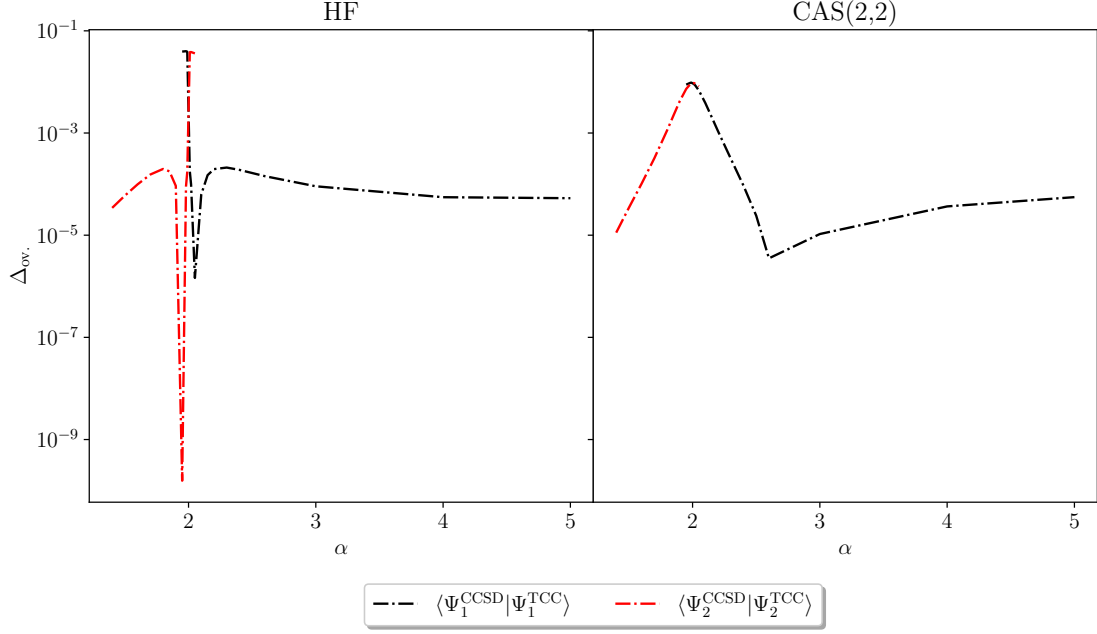


**Figure 5:** Overlap error  $\Delta_{ov.}$  of CCSD with TCCSD(2,2) based on the reference determinants  $\Phi_1$  and  $\Phi_2$  and different orbital bases: (1) HF orbitals (left) and CAS(2,2) orbitals (right).

the MR region.

The same applies to the calculations of the SR regions based on CAS(2,2)-optimized orbitals. The reason for the small overlap error is that the orbitals and active space amplitudes are optimized for the degenerate case, and these contribute most to the overlap between TCCSD and FCI. For reasons of completeness also the  $T_1$  and  $D_1$  diagnostics are shown in Figure 6. The  $T_1$  and  $D_1$  diagnostics mostly agree with the overlap diagnostics for SR-dominated regions. However, the  $T_1$  and  $D_1$  diagnostics below their thresholds in the range  $1.75 < \alpha < 2.25$  contradict the more reliable FCI overlap error, as they seem to predict that CCSD and TCCSD deliver a reliable wave function representation in that range, while in fact they do not. Since the overlap error with FCI provides more reliable diagnostics than the  $T_1$  and  $D_1$  values based on CASSCF orbitals, we only consider the overlap for the H8 model (see supporting information for  $T_1$  and  $D_1$  for H8). It should be noted, however, that  $T_1$  and  $D_1$  come with no additional computation overhead and are therefore a practical means

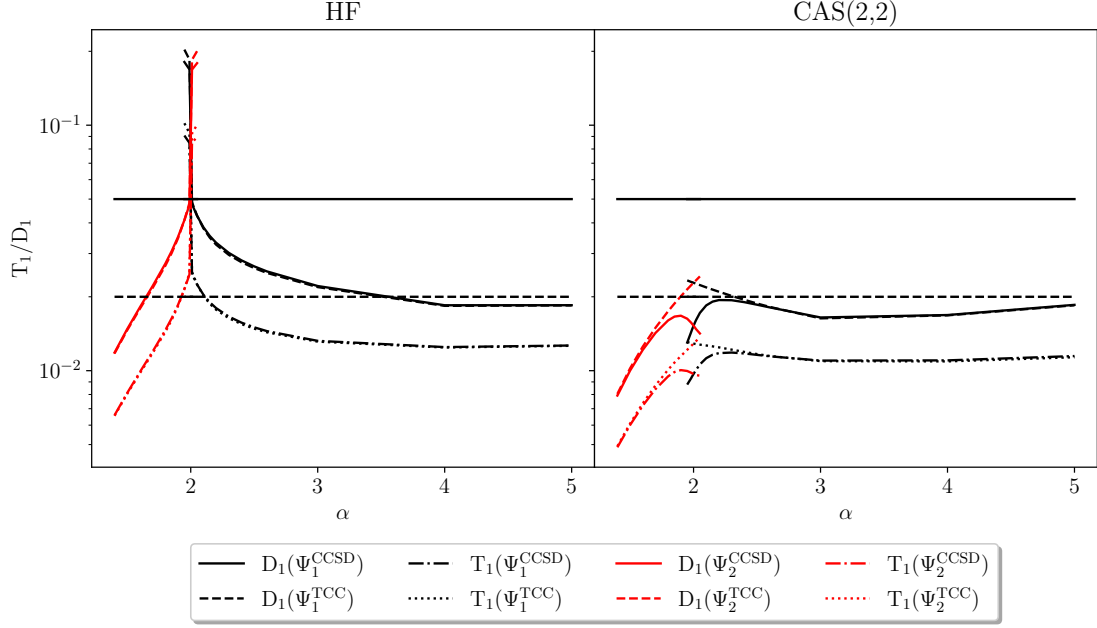


**Figure 6:**  $T_1$  and  $D_1$  diagnostics for the TCCSD(2,2) and CCSD wave function based on  $\Phi_1$  (black lines) and  $\Phi_2$  (red lines) and different orbital bases: (1) HF orbitals (left) and CAS(2,2) orbitals (right). The solid upper line represents the  $D_1$  reliability threshold, while the dotted line corresponds to the  $T_1$  reliability threshold.

to evaluate the quality of general SRCC wave functions.

### 3.3 H8 model

The H8 model system [78] consists of four hydrogen molecules with a constant intramolecular distance of 2 Bohr. The molecules are arranged in an octagonal configuration with  $D_{8h}$  symmetry. Two  $H_2$  units which lie on the top and bottom edge of the octagon remain fixed in their position. The distance between the units at the left and right edge can be controlled by the parameter  $\alpha$ , (see Figure 7). The variation of  $\alpha$  results in a compressed configuration for  $\alpha < 0$ , an octagonal configuration for  $\alpha = 0$  and a stretched configuration for  $\alpha > 0$ . The stretched and

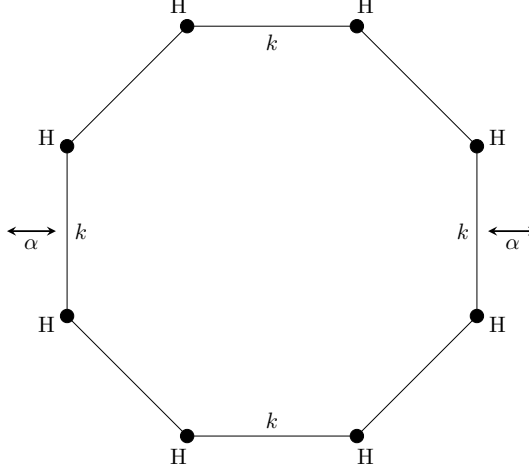


**Figure 7:** The H8 model consists of four stretched  $\text{H}_2$  units with a constant bond length  $k = 2$  Bohr. Two units lie on the top and bottom edges of the octagon and remain fixed in their position. The distance between the vertically arranged units can be controlled by the parameter  $\alpha$  which is characteristic for the distortion of the regular octagonal geometry.

compressed configuration corresponds to the  $D_{2h}$  symmetry, with

$$|\Phi_1\rangle = |(1a_g)^2(1b_{3u})^2(1b_{2u})^2(2a_g)^2\rangle, \quad (23)$$

$$|\Phi_2\rangle = |(1a_g)^2(1b_{3u})^2(1b_{2u})^2(1b_{1g})^2\rangle, \quad (24)$$

as the dominant reference determinants in short-hand notation (see supporting information for the complete set of HF orbitals). To attain a consistent description of the electronic ground state along the deformation of the H8 system, the active space is chosen to be  $\text{CAS}(2e^-, (2a_g)(1b_{1g}))$ . The octagonal configuration at  $\alpha = 0$  represents the completely symmetric, i.e.,  $D_{8h}$  configuration. Figure 8 shows the square of the  $c_0$  CI expansion coefficients for the two determinants.  $|\Phi_2\rangle$  represents the dominant determinant for  $\alpha < -0.1$  and  $|\Phi_1\rangle$  for  $\alpha > 0.1$ , while the weight of the determinants increases for  $-0.1 < \alpha < 0.1$  and becomes fully degenerate for  $\alpha = 0$ . Figure 9 shows the energy error for TCCSD(2,2) and CCSD with respect to FCI based on HF and CAS(2,2) orbitals. In the HF orbital basis, CCSD shows a much smaller energy error than TCCSD, in contrast to the energy error profile based on the CASSCF orbitals, where this is only valid only for  $\alpha < -0.05$  and  $\alpha > 0.05$ . Owing to the absolute value of the error, the spikes near  $\alpha = 0$  represent a sign

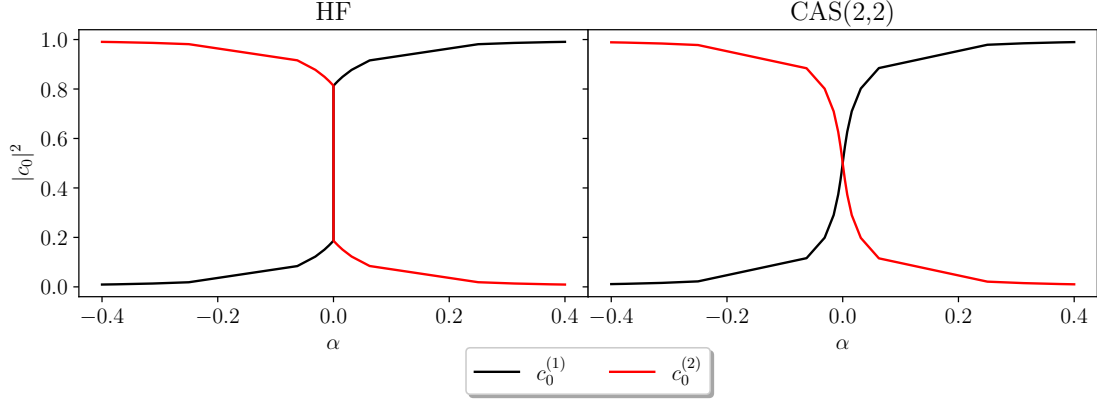


**Figure 8:** Square of the CI coefficient ( $|c_0|^2$ ) of  $\Phi_1$  ( $c_0^{(1)}$ ) and  $\Phi_2$  ( $c_0^{(2)}$ ) of Eqs. (23) and (24) for different values of  $\alpha$ . Both expansion coefficients were obtained for determinants constructed from different molecular orbital bases: (1) HF orbitals (left) and (2) CAS(2,2) orbitals (right).

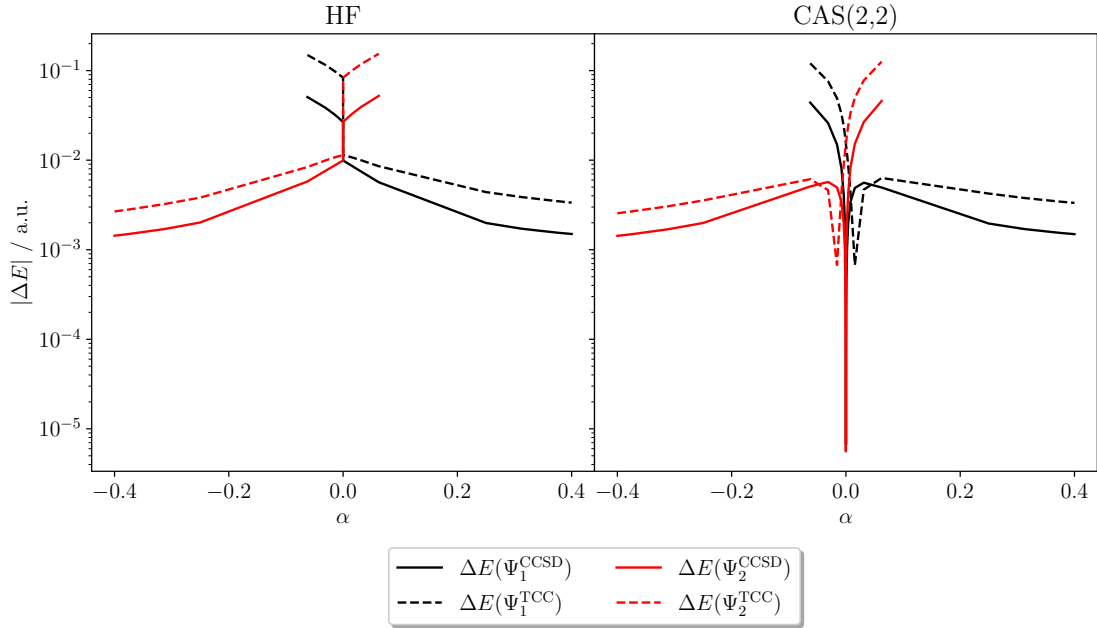


**Figure 9:** Absolute energy error  $|\Delta E|$  of TCCSD(2,2) and CCSD with respect to the FCI energy based on the reference determinant  $\Phi_1$  and  $\Phi_2$  and different orbital bases: (1) HF orbitals (left) and CAS(2,2) orbitals (right).

change in the error. Similar to the P4 model, the energy error increases with an

increasing MR-character of the wave function, but it is surprising that the TCCSD energy error for the high-symmetry configurations near  $\alpha = 0$ , which results in a strong multi-configurational character, is larger than for CCSD.

Because of the optimized CI coefficients in the CASSCF basis, TCCSD(2,2) yields a smaller energy error than CCSD for the near high-symmetry configurations near  $\alpha = 0$ . However, the effect of the amplitudes obtained from the active space is not enough to *tailor* the external amplitudes to describe the nearly degenerate configurations accurately. Because of the fixed CAS amplitudes, TCCSD shows a larger energy error than CCSD for the SR-dominated regions. This is supported by the

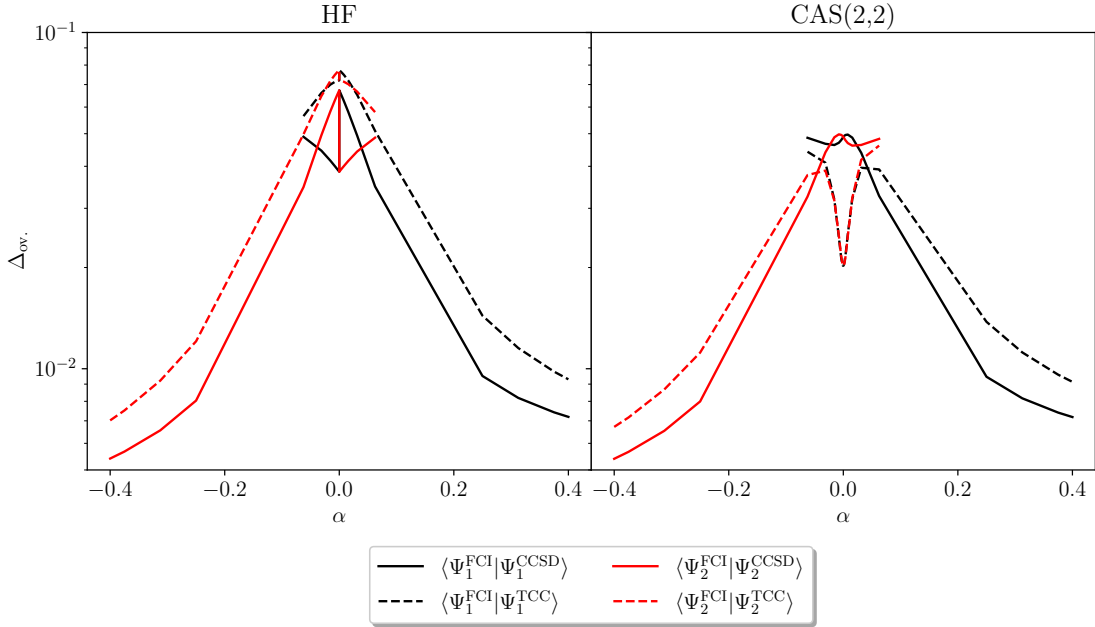


**Figure 10:** Overlap error  $\Delta_{ov.}$  of CCSD and TCCSD(2,2) with FCI, based on the reference determinants  $\Phi_1$  and  $\Phi_2$  and different orbital bases: (1) HF orbitals (left) and CAS(2,2) orbitals (right).

measurements of the overlap error in Figure 10. The HF orbital-based CCSD wave function shows for all values of  $\alpha$  a smaller overlap error than the TCCSD wave function. In the CASSCF orbital basis TCCSD yields a smaller overlap error for  $-0.05 < \alpha < 0.05$ . Also the TCCSD overlap errors of both TCCSD wave functions diverge only after this region. However, the overlap error for the MR region is rather

large for the CCSD and TCCSD wave functions compared to what we observed for P4 model and to the errors seen in the SR region.

From the  $c_0$  coefficients we can conclude, that the H8 model relies more on a MR description than the P4 model. In view of the overlap error it is clear that TCCSD requires a CAS optimized orbital basis in order to yield a smaller overlap error than CCSD for the MR region around  $\alpha = 0$ .

### 3.3.1 H8 CAS(8,8)

Faulstich *et al.* emphasized [70, 71] that in TCC, the active space must include all determinants that are mainly responsible for static correlation. A side effect of the large active space is also a partial reduction of the size-consistency error introduced by the truncation of the active space [69]. The entanglement dia-

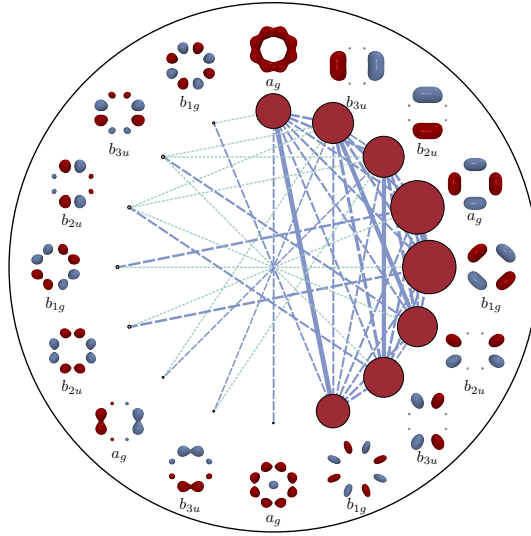


**Figure 11:** Entanglement diagram for the H8 model at  $\alpha = 0$  in the HF orbital basis. The size of the circles represents the single-orbital entropy defined in Eq. (18). The lines between the circles denote the mutual information of Eq. (19) with the thickness representing its magnitude.

gram in Figure 11 features large single-orbital entropies for the first eight orbitals and strong mutual information for these orbital pairs. Therefore, we recalculated

the H8 model with a CAS(8,8) to ensure that all strongly correlated orbitals are included in the active space. Figure 12 depicts the CI coefficients for the two

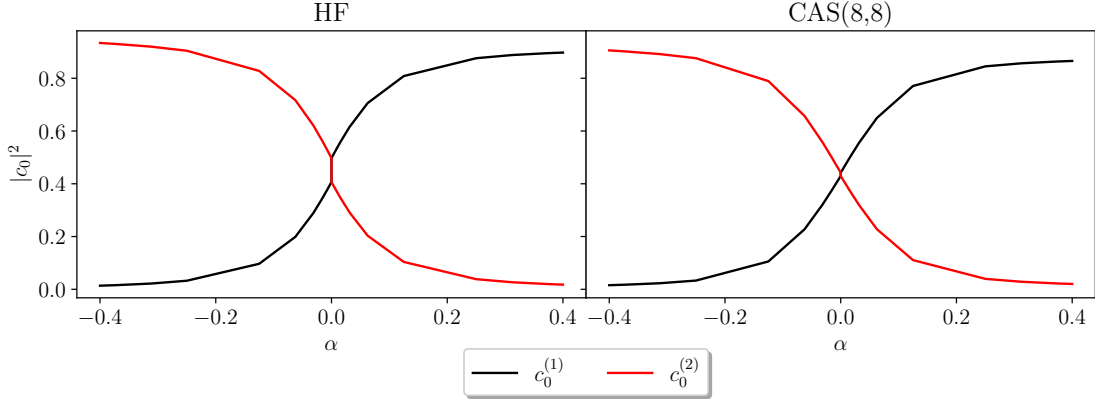


**Figure 12:** Square of the CI coefficient ( $|c_0|^2$ ) of  $\Phi_1$  ( $c_0^{(1)}$ ) and  $\Phi_2$  ( $c_0^{(2)}$ ) of Eqs. (23) and (24) for different values of  $\alpha$ . Both expansion coefficients were obtained for determinants constructed from different molecular orbital bases: (1) HF orbitals (left) and (2) CAS(2,2) orbitals (right).

most dominant reference determinants given in Eqs. (23) and (24) from a CAS(8  $e^-$ ,  $(1a_g)(1b_{2u})(1b_{3u})(2a_g)(1b_{1g})(2b_{2u})(2b_{3u})(2b_{1g})$ ) calculation (see Figure 11). Since the CAS(8,8) contains 4896 more determinants than the CAS(2,2) and the weight of the most dominant determinant is less than 0.9, this means that other determinants in the wave function also become important. In general the CI coefficients of the CAS(8,8) show the same behavior as for CAS(2,2) so that they become degenerate for  $\alpha = 0.0$ .

We performed the analysis of the H8 model with CAS(8,8) in analogy to the analysis for CAS(2,2). Accordingly, Figure 13 shows the absolute energy error with respect to FCI. From the absolute energy error we conclude that CCSD yields energies with a smaller energy error than TCCSD for the SR-dominated region ( $\alpha < -0.09, \alpha > 0.04$ ). In contrast to the smaller CAS, TCCSD provides energies with a smaller error than CCSD for the MR region, based on HF orbitals. However, for the calculations based on CAS(8,8) optimized orbitals, CCSD yields better energies than TCCSD for compressed configurations and for stretched configurations



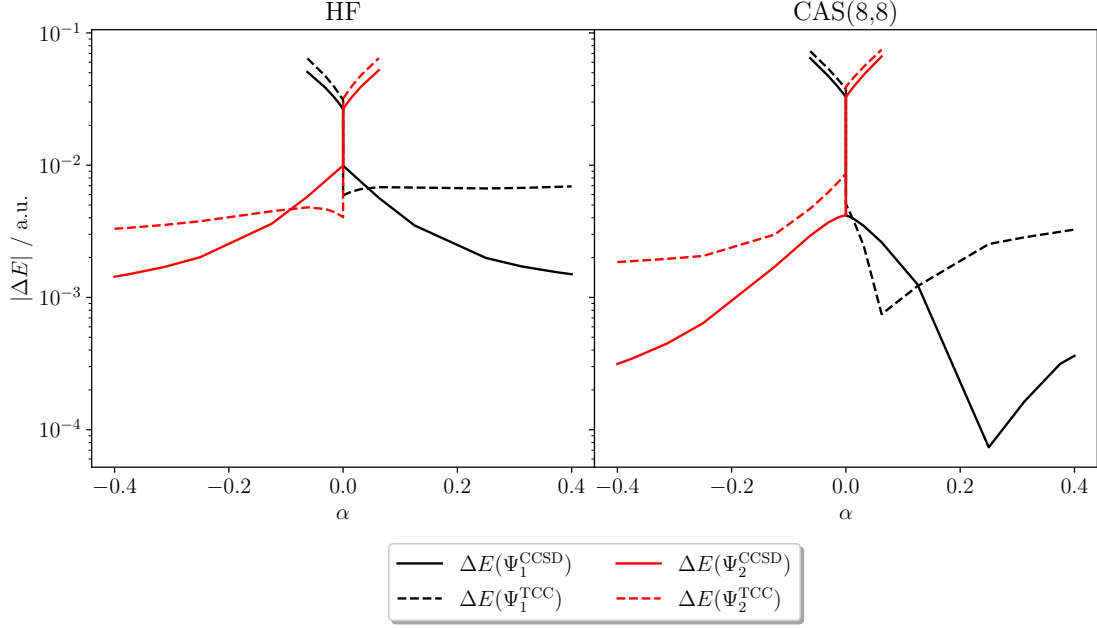


**Figure 13:** Absolute energy error  $|\Delta E|$  of TCCSD(8,8) and CCSD with respect to the FCI energy based on the reference determinant  $\Phi_1$  and  $\Phi_2$  and different orbital bases: (1) HF orbitals (left) and CAS(8,8) orbitals (right).

(with  $\alpha > 0.12$ ), whereas for configurations with  $0 < \alpha < 0.12$  TCCSD provides energies with a smaller energy error. Since neither CCSD, nor TCCSD are variational methods, the spikes in these diagrams correspond to sign changes in the error.

To gain more insight into the quality of the wave function, Figure 14 shows the overlap error of the wave functions with respect to FCI. Contrasting the energy error, TCCSD yields an improved wave function compared to CCSD for  $-0.23 < \alpha < 0.24$ . It is not surprising that a larger active space yields better wave function quality, since the coefficients which correspond to singly and doubly excited determinants were optimized with respect to highly excited determinants in the active space. But for configurations with nearly degenerate determinants, the overlap error is still above 0.02, which would not be the case for a *genuine* MR method. As expected, the CCSD wave functions feature larger overlaps with the exact reference for SR-dominated regions.

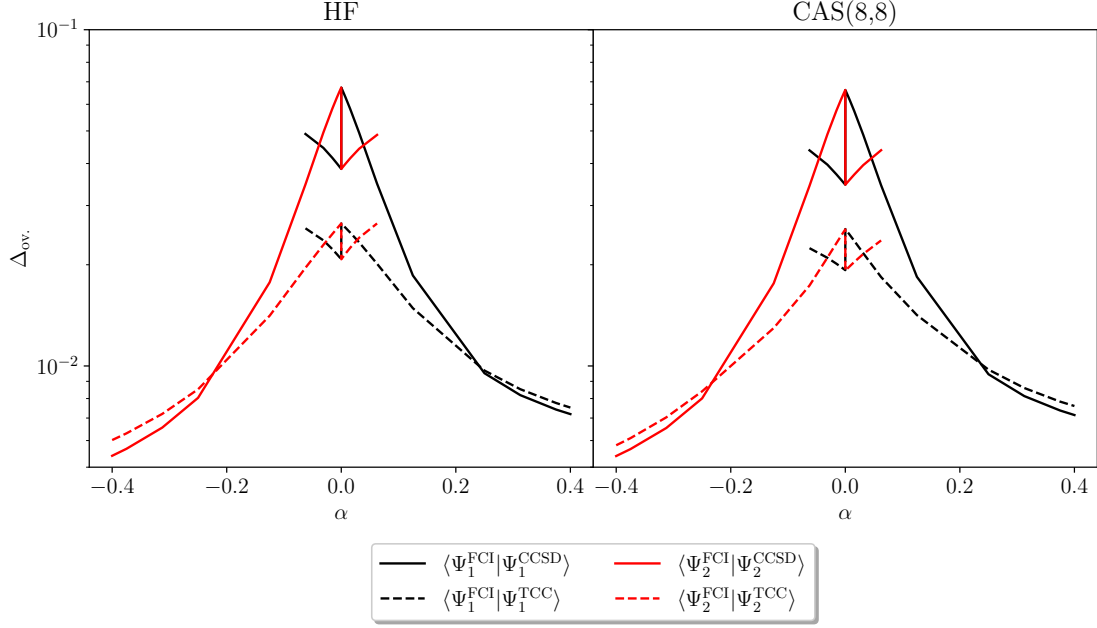


**Figure 14:** Overlap error  $\Delta_{\text{ov.}}$  of CCSD and TCCSD(8,8) with FCI, based on the reference determinants  $\Phi_1$  and  $\Phi_2$  and different orbital bases: (1) HF orbitals (left) and CAS(8,8) orbitals (right).

## 4 Conclusions

We presented an analysis of the tailored coupled cluster model TCCSD, which combines coefficients from a variational complete active space approach with a projective CCSD ansatz for the wave function. We compared energies and wave functions delivered by TCCSD with the exact results from FCI calculations for well-studied multi-hydrogen configurations that resemble different correlation regimes by changing a single structural parameter. We also compared with the single-reference CCSD model to understand the benefits and drawbacks of TCCSD in direct comparison to its SR reference. As orbital bases we inspected HF as well as CAS-optimized orbitals.

One issue of the *tailored* CC approach is the lack of size consistency, which is clear from the evaluation of the P4 energy error based on CASSCF orbitals. Unlike CCSD, which is size-consistent, the TCCSD results do not converge to the FCI reference

in the dissociation limit. Nevertheless, the overlap error decreases even though the energy error becomes almost constant at larger values of  $\alpha$  for the P4 model. However, in general, CCSD provides smaller overlap and energy errors for the dissociated configurations.

Due to the use of CAS amplitudes, TCCSD should capture static electron correlation in molecular structures which present (almost) degenerate determinants. For such configurations, TCCSD and CCSD results show a high dependency on the underlying orbital basis. While for HF orbitals, CCSD shows almost the same or even smaller errors compared to TCCSD, this changes for CASSCF orbitals, where the TCCSD energy and overlap errors become smaller than the corresponding ones for CCSD. Especially for the degenerate case of the H8 model with a CAS(8,8), TCCSD shows a decrease of the overlap error.

Since the active space amplitudes must not relax during the external amplitude optimization, the quality of TCCSD depends strictly on the choice of the active space. Therefore, we exploited an entropy entanglement analysis of all orbitals to identify the orbitals with largest entanglement, which are the strongly correlated ones to be included in the active space. In general, increased active orbital space sizes improved the TCCSD wave function, i.e., the overlap error decreased to a maximum of 0.02. Despite increasing the active space to half of the total number of orbitals in the H8 model in the DZ basis, TCCSD still showed a large overlap error in the MR region. Finally, we investigated the dependence on a reference determinant. Since none of the structure-dependent TCCSD results turns out to be smooth and continuous for the different reference determinants, it confirms and highlights the dependence of a single-reference wave functions. As a result, the TCCSD method delivers a symmetry-broken wave function. However, TCCSD can yield a wave function with a smaller overlap error than CCSD for systems with a small but non-negligible MR character, if the active space includes all strongly entangled orbitals. Hence, it can be used to recover dynamic correlation for CAS-type methods, if the active space is balanced—for which orbital entanglement in an automated scheme may be exploited [34, 36, 83]—even if this requires large active spaces.

We therefore find supporting evidence that TCCSD is an approach that improves on the CCSD ansatz for strongly correlated systems. Potential drawback are (i) a potentially large active space (due to many strongly entangled orbitals, which eventually will require modern CAS approaches such as DMRG [as in Ref. [69]] and FCIQMC), (ii) the requirement of CASSCF orbitals, and (iii) the fact that systems with a truly strong MR character may not be described properly. To further improve on the accuracy of TCCSD, it should be extended as to incorporate dynamic correlation effects in the orbitals of the active space. For instance, this may be accomplished by short-range dynamic correlation in the CAS orbital optimization [88–90] or by transcorrelation [91]. Work along these lines is currently in progress in our laboratory.

## Acknowledgement

This work was financially supported by the Swiss National Science Foundation (project no. 200021\_182400). L.F. acknowledges The Schrödinger fellowship (J 3935-N34) of the Austrian Science Foundation (FWF).

## References

- [1] Löwdin, P.-O. Correlation Problem in Many-Electron Quantum Mechanics I. Review of Different Approaches and Discussion of Some Current Ideas. *Adv. Chem. Phys.* **1958**, *2*, 207–322.
- [2] Bartlett, R. J.; Musiał, M. Coupled-cluster theory in quantum chemistry. *Rev. Mod. Phys.* **2007**, *79*, 291–352.
- [3] Coester, F. Bound states of a many-particle system. *Nucl. Phys.* **1958**, *7*, 421–424.

- [4] Coester, F.; Kümmel, H. Short-range correlations in nuclear wave functions. *Nucl. Phys.* **1960**, *17*, 477–485.
- [5] Čížek, J. On the Correlation Problem in Atomic and Molecular Systems. Calculation of Wavefunction Components in Ursell-Type Expansion Using Quantum-Field Theoretical Methods. *J. Chem. Phys.* **1966**, *45*, 4256–4266.
- [6] Paldus, J.; Čížek, J.; Shavitt, I. Correlation Problems in Atomic and Molecular Systems. IV. Extended Coupled-Pair Many-Electron Theory and Its Application to the  $\text{BH}_3$  Molecule. *Phys. Rev. A* **1972**, *5*, 50–67.
- [7] Bartlett, R. J. Many-Body Perturbation Theory and Coupled Cluster Theory for Electron Correlation in Molecules. *Annu. Rev. Phys. Chem.* **1981**, *32*, 359–401.
- [8] Taylor, P. R. In *Lect. Notes Quantum Chem. II Eur. Summer Sch. Quantum Chem.*; Roos, B. O., Ed.; Springer-Verlag, 1994; Vol. 64; pp 125–202.
- [9] Purvis III, G. D.; Bartlett, R. J. A full coupled-cluster singles and doubles model: The inclusion of disconnected triples. *J. Chem. Phys.* **1982**, *76*, 1910–1918.
- [10] Raghavachari, K.; Trucks, G. W.; Pople, J. A.; Head-Gordon, M. A fifth-order perturbation comparison of electron correlation theories. *Chem. Phys. Lett.* **1989**, *157*, 479–483.
- [11] Bartlett, R. J.; Watts, J.; Kucharski, S.; Noga, J. Non-iterative fifth-order triple and quadruple excitation energy corrections in correlated methods. *Chem. Phys. Lett.* **1990**, *165*, 513–522.
- [12] Roos, B. O.; Taylor, P. R.; Siegbahn, P. E. A complete active space SCF method (CASSCF) using a density matrix formulated super-CI approach. *Chem. Phys.* **1980**, *48*, 157–173.
- [13] White, S. R. Density matrix formulation for quantum renormalization groups. *Phys. Rev. Lett.* **1992**, *69*, 2863–2866.

- [14] White, S. R. Density-matrix algorithms for quantum renormalization groups. *Phys. Rev. B* **1993**, *48*, 10345–10356.
- [15] Legeza, Ö.; Noack, R.; Sólyom, J.; Tincani, L. In *Computational Many-Particle Physics*; Fehske, H., Schneider, R., Weiße, A., Eds.; Springer, Berlin, Heidelberg, 2008; Vol. 739; pp 653–664.
- [16] Chan, G. K. L.; Dorando, J. J.; Gosh, D.; Hachmann, J.; Neuscamman, E.; Wang, H.; Yanai, T. In *Front. Quantum Syst. Chem. Phys.*; Wilson, S., Grout, P., Delgado-Barrio, G., Maruani, J., P., P., Eds.; Springer Netherlands, 2008; pp 49–65.
- [17] Chan, G. K. L.; Zgid, D. The Density Matrix Renormalization Group in Quantum Chemistry. *Annu. Rep. Comput. Chem.* **2009**, *5*, 149–162.
- [18] Marti, K. H.; Reiher, M. The Density Matrix Renormalization Group Algorithm in Quantum Chemistry. *Z. Phys. Chem.* **2010**, *224*, 583–599.
- [19] Marti, K. H.; Reiher, M. New Electron Correlation Theories for Transition Metal Chemistry. *Phys. Chem. Chem. Phys.* **2011**, *13*, 6750–6759.
- [20] Chan, G. K. L.; Sharma, S. The Density Matrix Renormalization Group in Quantum Chemistry. *Annu. Rev. Phys. Chem.* **2011**, *62*, 465–481.
- [21] Schollwöck, U. The density-matrix renormalization group in the age of matrix product states. *Ann. Phys.* **2011**, *326*, 96–192.
- [22] Wouters, S.; Van Neck, D. The density matrix renormalization group for ab initio quantum chemistry. *Eur. Phys. J. D* **2014**, *68*, 272.
- [23] Kurashige, Y. Multireference electron correlation methods with density matrix renormalisation group reference functions. *Mol. Phys.* **2014**, *112*, 1485–1494.
- [24] Olivares-Amaya, R.; Hu, W.; Nakatani, N.; Sharma, S.; Yang, J.; Chan, G. K. L. The ab-initio density matrix renormalization group in practice. *J. Chem. Phys.* **2015**, *142*, 034102.

- [25] Szalay, S.; Pfeffer, M.; Murg, V.; Barcza, G.; Verstraete, F.; Schneider, R.; Legeza, Ö. Tensor product methods and entanglement optimization for *ab initio* quantum chemistry. *Int. J. Quantum Chem.* **2015**, *115*, 1342–1391.
- [26] Yanai, T.; Kurashige, Y.; Mizukami, W.; Chalupský, J.; Lan, T. N.; Saitow, M. Density matrix renormalization group for *ab initio* Calculations and associated dynamic correlation methods: A review of theory and applications. *Int. J. Quantum Chem.* **2014**, *115*, 283–299.
- [27] Knecht, S.; Hedegård, E. D.; Keller, S.; Kovyrshin, A.; Ma, Y.; Muolo, A.; Stein, C. J.; Reiher, M. New Approaches for *ab initio* Calculations of Molecules with Strong Electron Correlation. *CHIMIA Int. J. Chem.* **2016**, *70*, 244–251.
- [28] Baiardi, A.; Reiher, M. The density matrix renormalization group in chemistry and molecular physics: Recent developments and new challenges. *J. Chem. Phys.* **2020**, *152*, 040903.
- [29] Freitag, L.; Reiher, M. In *Quantum Chemistry and Dynamics of Excited States: Methods and Applications*; González, L., Lindh, R., Eds.; John Wiley & Sons Ltd., 2020; pp 207–246.
- [30] Booth, G. H.; Thom, A. J. W.; Alavi, A. Fermion Monte Carlo without fixed nodes: A game of life, death, and annihilation in Slater determinant space. *J. Chem. Phys.* **2009**, *131*, 054106.
- [31] Cleland, D.; Booth, G. H.; Alavi, A. Communications: Survival of the fittest: Accelerating convergence in full configuration-interaction quantum Monte Carlo. *J. Chem. Phys.* **2010**, *132*, 041103.
- [32] Boguslawski, K.; Tecmer, P.; Legeza, Ö.; Reiher, M. Entanglement measures for single- and multireference correlation effects. *J. Phys. Chem. Lett.* **2012**, *3*, 3129–3135.
- [33] Stein, C. J.; Reiher, M. Measuring multi-configurational character by orbital entanglement. *Mol. Phys.* **2017**, *115*, 2110–2119.

- [34] Stein, C. J.; Reiher, M. Automated Selection of Active Orbital Spaces. *J. Chem. Theory Comput.* **2016**, *12*, 1760–1771.
- [35] Stein, C. J.; von Burg, V.; Reiher, M. The Delicate Balance of Static and Dynamic Electron Correlation. *J. Chem. Theory Comput.* **2016**, *12*, 3764–3773.
- [36] Stein, C. J.; Reiher, M. Automated Identification of Relevant Frontier Orbitals for Chemical Compounds and Processes. *Chimia* **2017**, *71*, 170–176.
- [37] Mok, D. K.; Neumann, R.; Handy, N. C. Dynamical and nondynamical correlation. *J. Phys. Chem.* **1996**, *100*, 6225–6230.
- [38] Hollett, J. W.; McKemmish, L. K.; Gill, P. M. The nature of electron correlation in a dissociating bond. *J. Chem. Phys.* **2011**, *134*, 224103.
- [39] Evangelista, F. A. Alternative single-reference coupled cluster approaches for multireference problems: The simpler, the better. *J. Chem. Phys.* **2011**, *134*, 224102.
- [40] Meissner, L. Size-consistency corrections for configuration interaction calculations. *Chem. Phys. Lett.* **1988**, *146*, 204–210.
- [41] Lyakh, D. I.; Musiał, M.; Lotrich, V. F.; Bartlett, R. J. Multireference Nature of Chemistry: The Coupled-Cluster View. *Chem. Rev.* **2012**, *112*, 182–243.
- [42] Evangelista, F. A. Perspective: Multireference coupled cluster theories of dynamical electron correlation. *J. Chem. Phys.* **2018**, *149*, 030901.
- [43] Jeziorski, B.; Monkhorst, H. J. Coupled-cluster method for multideterminantal reference states. *Phys. Rev. A* **1981**, *24*, 1668–1681.
- [44] Haque, M. A.; Mukherjee, D. Application of cluster expansion techniques to open-shells: Calculation of difference energies. *J. Chem. Phys.* **1984**, *80*, 5058–5069.
- [45] Lindgren, I.; Mukherjee, D. On the connectivity criteria in the open-shell coupled-cluster theory for general model spaces. *Phys. Rep.* **1987**, *151*, 93–127.



- [46] Piecuch, P.; Paldus, J. Orthogonally spin-adapted multi-reference Hilbert space coupled-cluster formalism: diagrammatic formulation. *Theoret. Chim. Acta* **1992**, *83*, 69–103.
- [47] Jankowski, K.; Paldus, J.; Grabowski, I.; Kowalski, K. Applicability of valence-universal multireference coupled-cluster theories to quasidegenerate electronic states. I. Models involving at most two-body amplitudes. *J. Chem. Phys.* **1992**, *97*, 7600.
- [48] Paldus, J.; Piecuch, P.; Pylypow, L.; Jeziorski, B. Application of Hilbert-space coupled-cluster theory to simple  $(\text{H}_2)_2$  model systems: Planar models. *Phys. Rev. A* **1993**, *47*, 2738–2782.
- [49] Hanrath, M. Higher excitations for an exponential multireference wavefunction Ansatz and single-reference based multireference coupled cluster Ansatz: Application to model systems  $\text{H}_4$ ,  $\text{P}_4$ , and  $\text{BeH}_2$ . *J. Chem. Phys.* **2008**, *128*, 154118.
- [50] Evangelista, F. A.; Gauss, J. An orbital-invariant internally contracted multireference coupled cluster approach. *J. Chem. Phys.* **2011**, *134*, 114102.
- [51] Hanauer, M.; Köhn, A. Pilot applications of internally contracted multireference coupled cluster theory, and how to choose the cluster operator properly. *J. Chem. Phys.* **2011**, *134*, 204111.
- [52] Yanai, T.; Chan, G. K. L. Canonical transformation theory for multireference problems. *J. Chem. Phys.* **2006**, *124*, 194106.
- [53] Yanai, T.; Chan, G. K. L. Canonical transformation theory from extended normal ordering. *J. Chem. Phys.* **2007**, *127*, 104107.
- [54] Evangelista, F. A.; Gauss, J. On the approximation of the similarity-transformed Hamiltonian in single-reference and multireference coupled cluster theory. *Chem. Phys.* **2012**, *401*, 27–35.

- [55] Buenker, R. J.; Peyerimhoff, S. D.; Butscher, W. Applicability of the multi-reference double-excitation CI (MRD-CI) method to the calculation of electronic wavefunctions and comparison with related techniques. *Mol. Phys.* **1978**, *35*, 771–791.
- [56] Langhoff, S. R.; Davidson, E. R. Configuration interaction calculations on the nitrogen molecule. *Int. J. Quantum Chem.* **1974**, *8*, 61–72.
- [57] Andersson, K.; Malmqvist, P. Å.; Roos, B. O.; Sadlej, A. J.; Wolinski, K. Second-order perturbation theory with a CASSCF reference function. *J. Phys. Chem.* **1990**, *94*, 5483–5488.
- [58] Angeli, C.; Cimiraglia, R.; Evangelisti, S.; Leininger, T.; Malrieu, J.-P. Introduction of  $n$ -electron valence states for multireference perturbation theory. *J. Chem. Phys.* **2001**, *114*, 10252.
- [59] Angeli, C.; Cimiraglia, R.; Malrieu, J.-P.  $N$ -electron valence state perturbation theory: A fast implementation of the strongly contracted variant. *Chem. Phys. Lett.* **2001**, *350*, 297–305.
- [60] Oliphant, N.; Adamowicz, L. The implementation of the multireference coupled-cluster method based on the single-reference formalism. *J. Chem. Phys.* **1992**, *96*, 3739.
- [61] Piecuch, P.; Kowalski, K.; Pimienta, I. S. O.; Fan, P.-D.; Lodriguito, M.; McGuire, M. J.; Kucharski, S. A.; Kuś, M.; Musiał, M. Method of moments of coupled-cluster equations: a new formalism for designing accurate electronic structure methods for ground and excited states. *Theor. Chem. Acc.* **2004**, *112*, 349–393.
- [62] Kowalski, K.; Piecuch, P. Renormalized CCSD(T) and CCSD(TQ) approaches: Dissociation of the N<sub>2</sub> triple bond. *J. Chem. Phys.* **2000**, *113*, 5644.

- [63] Kowalski, K.; Piecuch, P. The method of moments of coupled-cluster equations and the renormalized CCSD[T], CCSD(T), CCSD(TQ), and CCSDT(Q) approaches. *J. Chem. Phys.* **2000**, *113*, 18.
- [64] Kinoshita, T.; Hino, O.; Bartlett, R. J. Coupled-cluster method tailored by configuration interaction. *J. Chem. Phys.* **2005**, *123*, 074106.
- [65] Hino, O.; Kinoshita, T.; Chan, G. K. L. Tailored coupled cluster singles and doubles method applied to calculations on molecular structure and harmonic vibrational frequencies of ozone. *J. Chem. Phys.* **2006**, *124*, 114311.
- [66] Lyakh, D. I.; Lotrich, V. F.; Bartlett, R. J. The ‘tailored’ CCSD(T) description of the automerization of cyclobutadiene. *Chem. Phys. Lett.* **2011**, *501*, 166–171.
- [67] Melnichuk, A.; Bartlett, R. J. Relaxed active space: Fixing tailored-CC with high order coupled cluster. I. *J. Chem. Phys.* **2012**, *137*, 214103.
- [68] Melnichuk, A.; Bartlett, R. J. Relaxed active space: Fixing tailored-CC with high order coupled cluster. II. *J. Chem. Phys.* **2014**, *140*, 064113.
- [69] Veis, L.; Anatalík, A.; Brabec, J.; Neese, F.; Legeza, Ö.; Pittner, J. Coupled Cluster Method with Single and Double Excitations Tailored by Matrix Product State Wave Functions. *J. Phys. Chem. Lett.* **2016**, *7*, 4072–4078.
- [70] Faulstich, F. M.; Laestadius, A.; Legeza, Ö.; Schneider, R.; Kvaal, S. Analysis of the Tailored Coupled-Cluster Method in Quantum Chemistry. *SIAM J. Numer. Anal.* **2019**, *57*, 2579–2607.
- [71] Faulstich, F. M.; Máté, M.; Laestadius, A.; Csirik, M. A.; Veis, L.; Antalík, A.; Brabec, J.; Schneider, R.; Pittner, J.; Kvaal, S.; Legeza, Ö. Numerical and Theoretical Aspects of the DMRG-TCC Method Exemplified by the Nitrogen Dimer. *J. Chem. Theory Comput.* **2019**, *15*, 2206–2220.
- [72] Lee, T. J.; Rice, J. E.; Scuseria, G. E.; Schaefer III, H. F. Theoretical investigations of molecules composed only of fluorine, oxygen and nitrogen: determination of the equilibrium structures of FOOF, (NO)<sub>2</sub> and FN<sub>2</sub> and the

- transition state structure for FNNF *cis-trans* isomerization. *Theoret. Chim. Acta* **1989**, *75*, 81–98.
- [73] Lee, T. J.; Taylor, P. R. A diagnostic for determining the quality of single-reference electron correlation methods. *Int. J. Quantum Chem.* **1989**, *36*, 199–207.
- [74] Janssen, C. L.; Nielsen, I. M. New diagnostics for coupled-cluster and Møller–Plesset perturbation theory. *Chem. Phys. Lett.* **1998**, *290*, 423–430.
- [75] Jankowski, K.; Kowalski, K. Approximate coupled cluster methods based on a split-amplitude strategy. *Chem. Phys. Lett.* **1996**, *256*, 141–148.
- [76] Kutzelnigg, W. Error analysis and improvements of coupled-cluster theory. *Theor. Chim. Acta* **1991**, *80*, 349–386.
- [77] Jankowski, K.; Paldus, J. Applicability of coupled-pair theories to quasidegenerate electronic states: A model study. *Int. J. Quantum Chem.* **1980**, *18*, 1243–1269.
- [78] Jankowski, K.; Meissner, L.; Wasilewski, J. Davidson-type corrections for quasidegenerate states. *Int. J. Quantum Chem.* **1985**, *28*, 931–942.
- [79] Sun, Q.; Berkelbach, T. C.; Blunt, N. S.; Booth, G. H.; Guo, S.; Li, Z.; Liu, J.; McClain, J. D.; Sayfutyarova, E. R.; Sharma, S.; Wouters, S.; Chan, G. K. PySCF: the Python-based simulations of chemistry framework. 2018.
- [80] Canal Neto, A.; Muniz, E.; Centoducatte, R.; Jorge, F. Gaussian basis sets for correlated wave functions. Hydrogen, helium, first- and second-row atoms. *J. Mol. Struct. THEOCHEM* **2005**, *718*, 219–224.
- [81] Dunning Jr., T. H. Gaussian Basis Functions for Use in Molecular Calculations. I. Contraction of (9s5p) Atomic Basis Sets for the First-Row Atoms. *J. Chem. Phys.* **1970**, *53*, 2823.

- [82] Dunning Jr., T. H.; Hay, P. J. In *Methods Electron. Struct. Theory*; Schaefer, H. F., Ed.; Plenum Press, New York, 1977; pp 1–27.
- [83] Stein, C. J.; Reiher, M. autoCAS: A Program for Fully Automated Multiconfigurational Calculations. *J. Comput. Chem.* **2019**, *40*, 2216–2226.
- [84] Legeza, Ö.; Sólyom, J. Optimizing the density-matrix renormalization group method using quantum information entropy. *Phys. Rev. B* **2003**, *68*, 195116.
- [85] Rissler, J.; Noack, R. M.; White, S. R. Measuring orbital interaction using quantum information theory. *Chem. Phys.* **2006**, *323*, 519–531.
- [86] Legeza, Ö.; Sólyom, J. Two-Site Entropy and Quantum Phase Transitions in Low-Dimensional Models. *Phys. Rev. Lett.* **2006**, *96*, 116401.
- [87] Boguslawski, K.; Tecmer, P. Orbital entanglement in quantum chemistry. *Int. J. Quantum Chem.* **2015**, *115*, 1289–1295.
- [88] Savin, A.; Flad, H.-J. Density functionals for the Yukawa electron-electron interaction. *Int. J. Quantum Chem.* **1995**, *56*, 327–332.
- [89] Fromager, E.; Toulouse, J.; Jensen, H. J. A. On the universality of the long-/short-range separation in multiconfigurational density-functional theory. *J. Chem. Phys.* **2007**, *126*, 074111.
- [90] Hedegård, E. D.; Olsen, J. M. H.; Knecht, S.; Kongsted, J.; Jensen, H. J. A. Polarizable embedding with a multiconfiguration short-range density functional theory linear response method. *J. Chem. Phys.* **2015**, *142*, 114113.
- [91] Baiardi, A.; Reiher, M. Transcorrelated Density Matrix Renormalization Group. 2020; arXiv:1910.00137.